BJP British Journal of Pharmacology

DOI:10.1111/bph.12201
www.brjpharmacol.org

RESEARCH PAPER

Identification through high-throughput screening of 4′-methoxyflavone and 3′,4′-dimethoxyflavone as novel neuroprotective inhibitors of parthanatos

A A Fatokun[1,2]*, J O Liu[3], V L Dawson[1,2,4,5] and T M Dawson[1,2,4]

[1]*Neuroregeneration and Stem Cell Programs, Institute for Cell Engineering, Johns Hopkins University School of Medicine, Baltimore, MD, USA,* [2]*Department of Neurology, Johns Hopkins University School of Medicine, Baltimore, MD, USA,* [3]*Departments of Oncology and Pharmacology, Johns Hopkins University School of Medicine, Baltimore, MD, USA,* [4]*Solomon H. Snyder Department of Neuroscience, Johns Hopkins University School of Medicine, Baltimore, MD, USA, and* [5]*Department of Physiology, Johns Hopkins University School of Medicine, Baltimore, MD, USA*

Correspondence
Amos A Fatokun, Institute of Cell Signalling, School of Biomedical Sciences, University of Nottingham Medical School, Nottingham NG7 2UH, UK. E-mail: amos.fatokun@nottingham.ac.uk or amosfatokun@yahoo.com; Valina L Dawson or Ted M Dawson, Institute for Cell Engineering, Johns Hopkins University School of Medicine, Edward D. Miller Research Building, 733 North Broadway, Baltimore, MD 21205, USA. E-mail: vdawson@jhmi.edu; tdawson@jhmi.edu

*Present address: Institute of Cell Signalling, School of Biomedical Sciences, University of Nottingham Medical School, Queen's Medical Centre, Nottingham NG7 2UH, UK. Tel.: +44 115 823 0080; Fax: +44 115 823 0081.

Keywords
PARP-1 inhibitors; high-throughput screen; neurodegeneration; flavone; neurotherapeutics; methoxylation

Received
30 November 2012
Revised
2 March 2013
Accepted
10 March 2013

BACKGROUND AND PURPOSE

The current lack of disease-modifying therapeutics to manage neurological and neurodegenerative conditions justifies the development of more efficacious agents. One distinct pathway leading to neuronal death in these conditions and which represents a very promising and attractive therapeutic target is parthanatos, involving overactivation of PARP-1. We therefore sought to identify small molecules that could be neuroprotective by targeting the pathway.

EXPERIMENTAL APPROACH

Using HeLa cells, we developed and optimized an assay for high-throughput screening of about 5120 small molecules. Structure–activity relationship (SAR) study was carried out in HeLa and SH-SY5Y cells for molecules related to the initial active compound. The neuroprotective ability of each active compound was tested in cortical neuronal cultures.

KEY RESULTS

4′-Methoxyflavone (4MF) showed activity by preventing the decrease in cell viability of HeLa and SH-SY5Y cells caused by the DNA-alkylating agent, *N*-methyl-*N*′-nitro-*N*-nitrosoguanidine (MNNG), which induces parthanatos. A similar compound from the SAR study, 3′,4′-dimethoxyflavone (DMF), also showed significant activity. Both compounds reduced the synthesis and accumulation of poly (ADP-ribose) polymer and protected cortical neurones against cell death induced by NMDA.

CONCLUSIONS AND IMPLICATIONS

Our data reveal additional neuroprotective members of the flavone class of flavonoids and show that methoxylation of the parent flavone structure at position 4′ confers parthanatos-inhibiting activity while additional methoxylation at position 3′, reported by others to improve metabolic stability, does not destroy the activity. These molecules may therefore serve as leads for the development of novel neurotherapeutics for the management of neurological and neurodegenerative conditions.

Abbreviations

4MF, 4′-methoxyflavone; 5F2DU, 5-fluoro-2′-deoxyuridine; AB, alamar blue; AIF, apoptosis-inducing factor; CSS, control salt solution; CTG, CellTiter-Glo; CV, coefficient of variation; DMF, 3′,4′-dimethoxyflavone; DMSO, dimethyl sulfoxide; DPQ, 3,4-dihydro-5-[4-(1-piperidinyl)butoxyl]-1(2H)-isoquinolinone; HTS, high-throughput screening; JHDL, Johns Hopkins Drug Library; MEM, minimum essential medium; MNNG, *N*-methyl-*N*′-nitro-*N*-nitrosoguanidine; MSSPL, MSSP (Spectrum2K) Library; P/S, penicillin–streptomycin; S/B, signal-to-background; SAR, structure-activity relationship; z-VAD-fmk, benzyloxycarbonyl-Val-Ala-Asp(OMe)-fluoromethylketone

Introduction

The current burden of CNS diseases is significant, and a number of these afflictions, such as stroke, are among the leading causes of death, especially in the developed world (Liang *et al.*, 2004). The grim prospect of an unprecedented explosion in the incidence of these disorders calls for renewed efforts to identify novel and more efficacious agents for their management (Dawson and Dawson, 2004), which, unfortunately, are not available to date.

Research in neurotherapeutics development is now focused on well-defined or emerging signalling pathways, assays to study which can be miniaturized for high-throughput screening (HTS) of compound libraries. One major pathway now identified to be involved in the death of neurones in stroke and neurodegenerative diseases involves the overactivation of the nuclear enzyme, PARP (Yu *et al.*, 2002). This leads to the production of its polymer product, poly (ADP-ribose) (PAR), which has been shown to be directly toxic to neurones (Andrabi *et al.*, 2006). Although there are now at least 18 members of the PARP protein family, PARP-1 (116 KDa) produces over 95% of the total PAR polymer in most cells (Dawson and Dawson, 2004), which is why most attention is focused on this isoform. PAR signals to a mitochondrially localized protein, apoptosis-inducing factor (AIF), compelling it to translocate to the nucleus, where it (AIF) causes large-scale (50 kb) DNA fragmentation and nuclear condensation (Yu *et al.*, 2002). This stage is the commitment point for cell death in several models of neurotoxicity, and it has been shown that AIF has the ability to mediate directly the toxicity of PAR polymer (Yu *et al.*, 2006). The involvement of both PARP-1 activation and the consequent nuclear AIF translocation has been demonstrated in models of stroke (Li *et al.*, 2007), traumatic brain injury (Zhang *et al.*, 2002), neurodegeneration (Yu *et al.*, 2003), heart ischaemia-reperfusion injury (Song *et al.*, 2008) and many other pathologies (Virag, 2005). We have termed this cell-death pathway 'parthanatos' (Andrabi *et al.*, 2008), to distinguish it from other forms of cell death.

Typically, neurones could be buffeted by a myriad of insults that are capable of causing excessive DNA damage, such as ischaemia, excitotoxicity, oxidative stress, nitrosative stress and inflammation. Some of these insults can elicit damage directly (e.g. oxidative stress), while some do so through excessive activation of the ionotropic NMDA receptor, triggering a cascade of highly choreographed pathological events, including, in sequence, excessive calcium influx, activation of neuronal NOS, production of nitric oxide and formation of the highly toxic peroxynitrite. Peroxynitrite induces pronounced DNA damage, thus sensitizing PARP-1 to produce prodigious amount of PAR polymer, leading to nuclear AIF translocation, large-scale DNA fragmentation and nuclear condensation, and, eventually, neuronal death (Yu *et al.*, 2002). The parthanatos cascade, therefore, represents a very attractive and promising therapeutic target.

We have attempted to identify novel blockers of the parthanatos cascade, hypothesizing that such molecules will be robustly neuroprotective and thus serve as leads for the development of more efficacious neuroprotectants. We exploited a unique biochemical feature of parthanatos – its resistance to caspase inhibition (Yu *et al.*, 2002) – to design an HTS assay, which was optimized and used to screen a few thousand compounds, from which we identified two compounds of the flavone family of flavonoids that showed novel activity as neuroprotective inhibitors of parthanatos. We found that methoxylation of flavone at the 3′ position confers ability to inhibit parthanatos while additional methoxylation at the 4′ position does not destroy this activity.

Materials and methods

Reagents and chemicals

Culture media, TrypLE™ Express, FBS, poly-L-ornithine and alamar blue (AB) were from Invitrogen (Carlsbad, CA, USA). CellTiter-Glo™ (CTG) was from Promega Incorporation (Madison, WI, USA). Horse serum was from Sigma-Aldrich (St. Louis, MO, USA); glutamine and penicillin–streptomycin (P/S) antibiotic were from Mediatech Inc. (Manassas, VA, USA). 3,4-Dihydro-5-[4-(1-piperidinyl)butoxyl]-1(2H)-isoquinolinone (DPQ) was from Sigma-Aldrich and Benzyloxycarbonyl-Val-Ala-Asp(OMe)-fluoromethylketone (z-VAD-fmk) was from both Sigma-Aldrich and R&D Systems (Minneapolis, MN, USA). *N*-methyl-*N*′-nitro-*N*-nitrosoguanidine (MNNG) was obtained from Chem Service (West Chester, PA, USA). Anti-PAR polyclonal primary antibody was from Trevigen (Gaithersburg, MD, USA), while anti-rabbit IgG secondary antibody and HRP-conjugated anti-β-actin antibody were from Sigma-Aldrich. MSSP Library (2 mM) was purchased from the Johns Hopkins ChemCORE Facility (10 mM stock was originally purchased from MicroSource Discovery Inc., Groton, CT, USA). Johns Hopkins Drug Library (JHDL) was supplied by one of the authors, Prof. Jun Liu. Flavonoid compounds and related chemicals were purchased from Indofine Chemicals (Hillsborough, NJ, USA), except wogonin, which was purchased from Sigma-Aldrich. Culture plates were from BD Falcon (Franklin Lakes, NJ, USA), except NUNC plates and specialized screening plates that were obtained from Fisher Scientific (Pittsburgh, PA, USA). Reagents and chemicals were properly stored.

Cell culture: cell lines and primary neuronal cultures

HeLa and SH-SY5Y cells were grown in DMEM supplemented with 10% FBS and 1% P/S antibiotic combination.

They were incubated at 37°C in a humidified atmosphere of 5% CO_2.

Primary neuronal cultures were prepared from gestational day 15–16 (E15-E16) fetal CD1 mice according to standard protocols as previously described (Dawson *et al.*, 1993). Experiments were performed in accordance with the National Institutes of Health Guidelines and approved by the Institutional Animal Care and Use Committee. Cultures were prepared and grown in minimum essential medium (MEM) supplemented with 20% horse serum, 3% 1 M D-glucose and 1% glutamine (designated 'mouse plating medium'). Inhibition of glial proliferation was achieved by addition to the growth medium at 3–4 days *in vitro* of 5-fluoro-2′-deoxyuridine (5F2DU, Sigma-Aldrich; 30 μM), prepared in mouse plating medium but with reduced (10%) horse serum supplementation (designated 'mouse feeding medium'). Cultures so treated represent 80–90% neurones. Experiments were conducted in 12-well NUNC plates previously coated with polyornithine (0.1 mg·mL^{-1}) to enhance cell attachment. Cultures were incubated at 37°C in a humidified atmosphere of 7% CO_2 (this slightly more acidic condition, compared with 5% CO_2, produces a pH of between 7.2 and 7.3, which favours neuronal growth in particular).

Assay development and optimization for HTS

Assay development and optimization were conducted in normal or specialized (fluorescence or luminescence) 96-well flat-bottom plates, into which 100 μL of cells was seeded per well. Cultures were allowed to adhere overnight and treated in multiple wells with MNNG (50 μM, prepared fresh every 15 min in DMEM) for 25 min (a condition which selectively induced parthanatos) in the presence or absence of each tested compound or condition. They were then incubated overnight (15–20 h) in the presence of each tested compound before cell viability was assessed as the end point, drawing from our previous findings that the toxic insult MNNG reduces the survival of HeLa cells through PARP-1 overactivation and this effect is significantly attenuated by DPQ, but not affected by z-VAD-fmk (Yu *et al.*, 2002).

For the primary screen, AB was used to assess cell viability. AB is added to cells in a single step, and the extent of its reduction, indicated by a colour change (blue to red), is proportional to the number of living cells. It has been successfully employed to quantify cell viability in HTS campaigns (e.g. see Sykes and Avery, 2009). Pre-warmed AB was added to cultures at 10% v/v and plates were incubated for 3 h at 37°C. They were then left at room temperature for 20 min and the dye's fluorescence was determined with a fluorometer at an excitation of 530 nm and an emission of 590 nm, using the XFluor4SafireII (version V 4.62b) software (Tecan, Männedorf, Switzerland). To optimize the use of AB, a range of cell densities (1×10^4–2×10^5 cells·mL^{-1}) and durations of incubation (2–9 h) were initially tested as recommended. A seeding density of 5000 cells per well for an incubation duration of 3 h was eventually chosen as the optimal working condition.

In order to assess HTS readiness and robustness of our assay, several parameters were quantified as follows:

Coefficient of Variation (CV) = SD/Average × 100

Signal-to-Background ratio (S/B) = Average/SD

Z′factor $= 1 - 3(S_{c^+} + S_{c^-})/(m_{c^+} - m_{c^-})$, where m_{c^+} and m_{c^-} are the mean values of signal of the positive control (DPQ in this case) and the negative control (z-VAD-fmk in this case) in the assay, and S_{c^+} and S_{c^-} are the standard deviations of the positive and negative controls (Zhang *et al.*, 1999), respectively.

An HTS-ready assay would have a CV of less than 10, an S/B ratio of at least 5 and a Z′ factor of between 0.5 and 1. Other parameters assessed include intra- and inter-plate and day-to-day variations, dimethyl sulfoxide (DMSO) tolerance and stability of reagents to storage and assay conditions. All parameters were optimized and number of assay steps reduced to the barest minimum.

For the secondary screen, the CTG luminescent cell viability assay was used. This assay makes use of the luciferase reaction to quantify ATP, a global indicator of cellular metabolism. The luminescent signal is proportional to the amount of ATP in cells. The simple and rapid nature of the method enables a single-step addition of the reagent directly to the cultured cells (Lovborg *et al.*, 2002). Treated culture plates were maintained at room temperature for 30 min, after which the re-constituted CTG reagent was added to each well at a 1:1 ratio. Plates were agitated for 2 min on an orbital shaker to lyse the cells and left at room temperature for 10 min to stabilize the luminescence signal (signal half-life >5 h). Plates were then read with a luminometer, using the software XFluor4SafireII (Version V 4.62b).

High-throughput screen of compound libraries

For the screening of the MSSP library (MSSPL), HeLa cells were seeded at 5000 cells per well (100 μL per well) into 25 BD Falcon™ (BD Biosciences, Bedford, MA, USA) 96-well black/clear, tissue culture-treated, flat-bottom plates, incubated and allowed to adhere overnight. Microscopic examination confirmed that the cultures were healthy and uncontaminated. Working compound plates were prepared in DMSO as 2 mM dilutions of the 10 mM master plates. The MSSPL contains 2000 compounds in 25 plates, with 80 compounds in each plate. The columns on the right and left sides of each plate (columns 1 and 12) contain DMSO only. They were therefore used for the assessment, in corresponding culture plates, of DMSO control treatment (column 1, top 4 wells), MNNG only-treatment (column 1, bottom 4 wells), MNNG treatment in the presence of positive control (DPQ, 30 μM) (column 12, top 4 wells) and MNNG treatment in the presence of negative control (Z-VAD-fmk, 100 μM) (column 12, bottom 4 wells). Corresponding compound plates (colourless) and culture plates (black) were labelled with the same identification number, from 1 to 25.

Compounds for addition to cultures were prepared in growth medium to a final concentration of 10 μM with the aid of CyBi™-well Liquid Handler (CyBio AG, Jena, Germany). MNNG was prepared at 11× concentration (550 μM) in DMEM every 15 min, and with the aid of the Multi-Drop Combi Liquid Dispenser (Thermo Fisher Scientific, Hudson, NH, USA), 10 μL was dispensed into each well to achieve a final concentration of 50 μM [same concentration (100%) and volume of DMSO dispensed into normal control wells]. Plates were shaken gently and briefly and incubated for 25 min. The entire content of each plate was

then dumped and medium from corresponding plates containing library or control compounds added by the use of the Liquid Handler. Each library compound was tested in a single well. Plates were then incubated overnight. AB was added to each well with the aid of the Multi-Drop Combi Liquid Dispenser. Plates were returned to the incubator for 3 h, after which they were allowed to equilibrate at room temperature for 20 min. The 25 plates, tagged for automated identification, were then stacked in a Twister II Plate Handler (Zymark Corporation, Hopkinton, MA, USA). Fluorescence for each plate was read using the Tecan microplate reader with the XFluor4SafireII software, generating data automatically in an Excel spreadsheet. These data were analysed by comparing fluorescence value in the presence of each compound (or average fluorescence value in case of DPQ or z-VAD-fmk) to average fluorescence value for the four normal control wells per plate.

The JHDL was screened in a way similar to the MSSPL's screen, but manually. A total of 3120 compounds (80 compounds per plate) were contained in 42 plates. Columns 1 and 12 of the stock (2 mM) compound plates contained DMSO only and corresponding positions in the culture plates were used for assessing the effect of DMSO only, as well as the effects of MNNG in the presence or absence of the positive and negative controls. The manual screening was executed in four project batches.

Assembly and screening of customized library

Each of the 27 compounds was prepared in DMSO as a 10 mM stock and diluted to 2 mM (with DMSO). Cells (HeLa, SH-SY5Y) were seeded into 96-well white, tissue culture-treated, flat-bottom plates suitable for luminescence reading. Screening was performed manually at 1, 10 and 20 μM of the compounds. Viability was determined using the CTG reagent. When hydrogen peroxide was used, cells were exposed to it at 2 mM for 2 h.

Immunoblot analysis

Treated cultures were washed twice with cold PBS and lysed by the addition of sample loading buffer (Laemmli sample buffer, with 2-mercaptoethanol added) containing SDS. Lysed samples were boiled on a heating block at 100°C for 5 min, and 20 μL was loaded onto 8% SDS-PAGE gel and electrophoresed in standard running buffer at 120 V for 1–1.5 h. Protein marker (Precision Plus Protein Standard, Biorad, Hercules, CA, USA) was included. The separated proteins were transferred electrophoretically to a nitrocellulose membrane (run at 120 V for 1.5 h in transfer buffer containing 10% of 10× Tris-glycine stock and 20% methanol). Non-specific binding was blocked by 1 h incubation with 5% non-fat dry milk. This was followed by overnight incubation on a slowly rotating shaker at 4°C with anti-PAR rabbit polyclonal primary antibody (1:10 000; Trevigen, Gaithersburg, MD, USA), prepared in 1% non-fat dry milk, with 0.01% w/v sodium azide added. Non-fat dry milk was prepared in PBS containing 0.1% Tween 20 (PBS-T). Blots were then washed with three 5 min changes of PBS-T and incubated for 1 h at room temperature with anti-rabbit IgG (whole molecule) – peroxidase secondary antibody (produced in goat; 1:5000; Sigma-Aldrich), prepared in 1% non-fat dry milk. Afterwards, blots were washed with three 10 min changes of PBS-T (blots placed on a fast-rotating shaker) and signals were detected by chemiluminescence using SuperSignal West Pico Chemiluminescent Substrate (Pierce, Rockford, IL, USA). Immunoblots were visualized on x-ray films. β-Actin was used as a loading control. To probe for β-actin, blots were incubated for 30 min with stripping buffer (Restore PLUS Western Blot Stripping Buffer, Thermo Scientific, Rockford, IL, USA), washed thrice with PBS-T, incubated with 5% non-fat dry milk for 1 h and then with HRP-conjugated anti-β-actin antibody for 1 h, after which signals were detected by chemiluminescence and visualized on x-ray films.

Induction of neuronal death

Cultures were used for experiments at 12–14 days *in vitro*. Control cultures were treated with control salt solution (CSS) containing 120 mM NaCl, 5.4 mM KCl, 1.8 mM $CaCl_2$, 25 mM Tris-HCl, pH 7.4, and 20 mM D-glucose. NMDA was always freshly prepared in CSS, with 10 μM glycine added to act as a co-agonist at the NMDA receptor. Each treatment lasted 5 min. Growth medium (conditioned) was first aspirated (and saved). Cultures were then washed with CSS and treated with CSS, NMDA or NMDA in the presence of the tested compounds, added concomitantly with NMDA and also included in the conditioned growth medium for restoration following NMDA treatment. The treatment conditions were such that NMDA selectively induced parthanatos, as earlier reported (Yu *et al.*, 2002). To control for any potential effect of DMSO employed as the vehicle for the chemical compounds, an equivalent volume of DMSO for the highest concentration of the tested compounds was added to CSS only-treated or NMDA only-treated cultures. After treatment, cultures were washed once with CSS, restored to the conditioned growth medium containing control or tested compounds and incubated for 15–20 h.

Assessment of cell death

Treated cultures were stained with Hoechst 33342 (5 $mg \cdot mL^{-1}$, labels all cells blue) for 5 min and propidium iodide (1 $mg \cdot mL^{-1}$, labels dead cells red) for a further 5 min. Medium was then aspirated and cultures were washed with, and maintained in, CSS before image acquisition. Plates were placed on the mechanized stage of a Zeiss microscope and images acquired with the ×20 objective (Hoechst: DAPI channel and PI: rhodamine channel) and saved. Computer-assisted cell counting was then performed with the aid of specialized software (Axiovision 4.6, Zeiss, Jena, Germany). At least three separate representative fields were counted for each treatment. Cell death was calculated as the ratio of PI-positive (red) cells to Hoechst 33342-positive (blue) cells, expressed as a percentage.

Statistics

Data are expressed as mean ± SEM. Data were either normalized to the control or to a given reference treatment, or stated as absolute values. For comparison of more than two means, one-way ANOVA was used, followed by either the Dunnett's (comparison with control) or the Student–Newman–Keuls' *post hoc* test, and a P-value of <0.05 was considered statistically significant.

Results

Development and optimization of a high-throughput primary assay to identify inhibitors of parthanatos

The flow chart of the experimental steps for the screening project is shown in Figure 1. MNNG was adopted as the stimulus for parthanatos, having been previously shown to kill HeLa cells, under the treatment conditions adopted, specifically in a PARP–1-dependent, caspase-independent manner requiring AIF translocation (Yu *et al.*, 2002). The PARP-1 inhibitor, DPQ (30 μM), and the pan-caspase inhibitor, z-VAD-fmk (100 μM), were chosen as positive and negative controls, respectively. DPQ significantly protects against the reduction in cell viability induced by MNNG, while z-VAD-fmk has no effect, and neither DPQ nor z-VAD-fmk has any effect on its own (Figure 2A). We show that AB adequately quantifies the concentration- and time-dependent reduction in HeLa cell viability induced by increasing concentrations of MNNG (25–100 μM), from 3 to 20 h following restoration to growth medium after 25 min of exposure to the toxin (Figure 2B). Similarly, cell viability following exposure to another toxin, hydrogen peroxide (0.25–4 mM), for up to 2 h, was shown by AB quantification to be decreased in a concentration- and time-dependent fashion (Figure 2C).

To optimize our assay for robustness for HTS, standard parameters were determined, including plate-to-plate and day-to-day variations, signal-to-background (S/B) ratio, coefficient of variation (CV) and Z′ factor. Variations within and between plates and between days were very minimal. Whereas MNNG reduced cell viability significantly, against which DPQ protected, but z-VAD lacked any effect, variations between the 2 days of experiment were insignificant (data not shown). The Z′ factors were within the 0.5–1 range, commonly taken as index of assay readiness for HTS. DMSO up to 1% had no effect on cell viability (data not shown).

To reduce the number of screening steps and cost, we tested whether protection against MNNG could be achieved by adding DPQ to the recovery medium only (i.e. after exposure to MNNG), rather than adding it before, during and after MNNG exposure. The presence of DPQ in the recovery medium only was sufficient to elicit protection (Figure 2D–F). This model was therefore adopted for HTS, thus reducing screening steps and project cost considerably by affording addition of each tested compound once, rather than thrice.

An initial small library of 84 kinase and phosphatase inhibitors (BIOMOL) was screened at 5 and 20 μM, and the assay was able to pick up differential effects of the various compounds tested, although no compound from the library significantly protected against MNNG effect (data not shown).

High-throughput screen identifies 4′-methoxyflavone (4MF) as protective against MNNG

We used our primary assay to screen two chemical libraries at a final concentration of 10 μM – MSSP (Spectrum2K) library (MSSPL) and JHDL. MSSPL has 2000 compounds (50% drug components, 30% natural products and 20% other bioactives), while JHDL is a collection of about 3120 drugs approved by US Food and Drug Administration or its foreign counterparts or drugs that have entered phase II clinical trials (Chong *et al.*, 2007; an overall total of about 5120 small molecules). Figure 3A and B show the results of the HTS for the MSSPL and the JHDL, respectively. Small molecules from MSSPL were contained in 25 plates while those from JHDL were contained in 42 plates, so values shown in Figure 3A and B were normalized to a set value of 40% for the effect of MNNG on viability in each plate. Z′ factors for MSSPL and JHDL were within the acceptable range, the positive control (DPQ) elicited protective response, while the negative control (z-VAD) had no effect. The overall pooled data in each case mimicked our standard model (Figure 3C and D, respectively), with an average Z′ factor of 0.7 in each case. Plates 19, 21 and 25 from the MSSPL were rescreened because of some deviations shown in the effects of MNNG, DPQ or z-VAD. Compounds toxic in the initial screen were rescreened at lower concentrations (2 and 5 μM) while those with borderline protection were rescreened at 20 μM.

Our selection criterion defined a hit as any compound that gave a normalized value of at least 60%, that is, at least 20% above the normalized value for the effect of MNNG alone. Based on this criterion, we identified 10 hits from the primary screen (0.2% hit rate), seven of them from the MSSPL [plate identification (ID) numbers: 2F08, 3B04, 3B06, 3C06, 3C07, 3D05, 3H05] and three from the JHDL (ID: 11E5, 16F10, 37C4). The effects of these compounds on MNNG toxicity are as shown in Figure 4A. Subsequent screens of initially toxic or marginally protective compounds at lower or higher concentrations, respectively, yielded no hits. Of all the 10 hits from the primary screen, 2F08 from the MSSPL elicited the highest protective effect against MNNG and was the only compound that retained its robust protection following confirmatory repeat screens (data not shown); it was thus confirmed as a true hit. 2F08 was identified as 4MF, a member of the flavone class of bioflavonoids. The structure of 4MF is shown in Figure 4B. The effect of 4MF was concentration-dependent, peaking at 25 μM (Figure 4C), with an EC_{50} value of 10.41 ± 1.31 μM (Figure 4D).

Secondary screen of customized flavonoid library

We examined whether the protective effect of 4MF was shared by other compounds of the same or similar chemical classes. We customized a small library of 27 flavonoids, including flavones carrying the hydroxy- or methoxy-substitutions, or both, to different degrees (up to penta-substitutions) and in different positions on the parent flavone structure (Figures 4E and 5, Supporting Information Table S1). The parent compound, flavone (Figure 4E), was included (to reveal any basal effect of the class), as were two non-flavone but polyphenolic compounds: epigallocatechin gallate, a flavanol, and resveratrol, a phytoalexin. 4MF was included as an internal control.

The luminescence-based assay (with the CTG reagent) used to assess cell viability was optimized for HTS. As shown in Figure 6A, MNNG reduced viability to about 12% of the control. The positive control DPQ protected significantly against the MNNG effect, raising cell viability to 86% of the control, but the negative control z-VAD had no effect (16% of

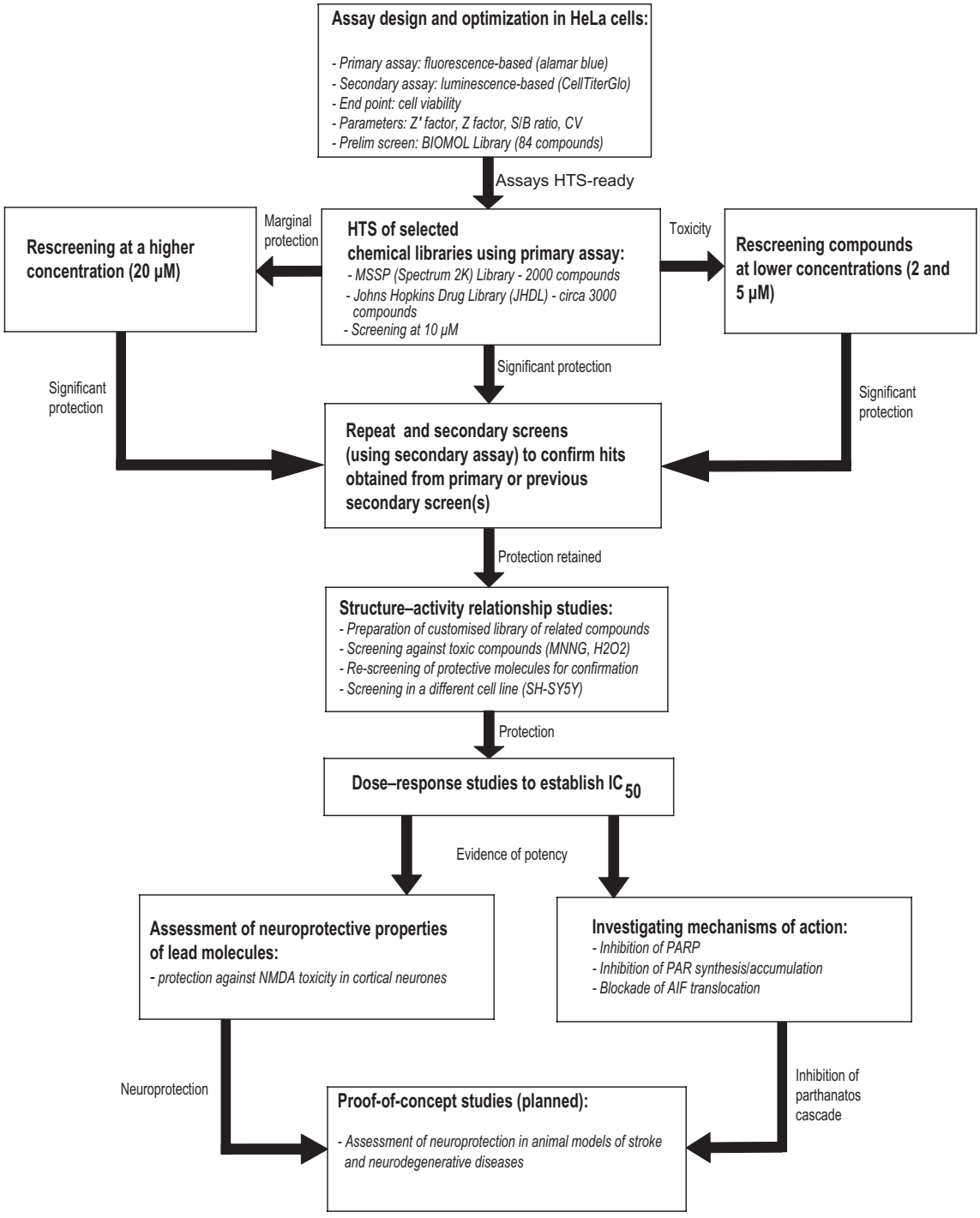

Figure 1

Flow chart for the screening project. Assay was developed and optimized in HeLa cells and then employed for high-throughput screen of two chemical libraries: the MSSP Library and the JHDL. AB (fluorescence-based) or CTG (luminescence-based) was used to quantify cell viability. Compounds showing toxicity were rescreened at 2 and 5 μM while those with marginal protective effects were rescreened at 20 μM. The 10 hits from the primary screen were rescreened for validation. One compound was confirmed as true hit. A number of small molecules belonging to the same class as this compound or similar classes were then selected and screened, resulting in one more hit that was then validated. Dose–response data were obtained for the two hits; they were proven to block the synthesis and accumulation of toxic PAR polymer and were also neuroprotective in cell culture. They are now to be investigated for their ability to afford neuroprotection in animal models of neuronal death.

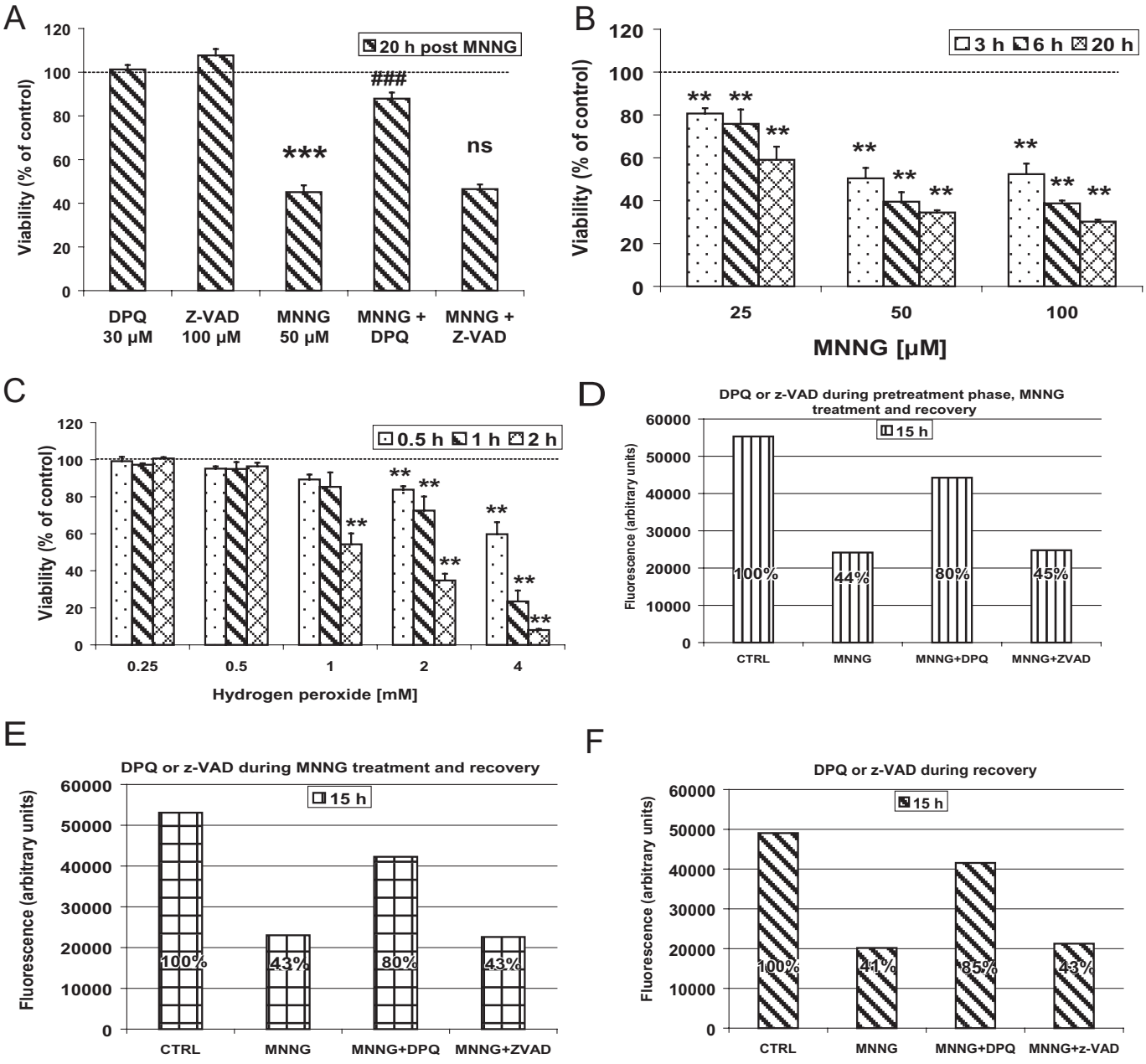

Figure 2

Assay development and optimization for high-throughput screen. (A) Model assay for the screening project. MNNG reduces cell viability significantly, protected against by DPQ (positive control), but not by Z-VAD-fmk (negative control), although neither control had any effect on its own. Viability was quantified 15–20 h after restoration of cultures to growth medium following 25 min exposure to MNNG (50 µM). (B) MNNG reduces cell viability in a concentration- and time-dependent manner, up to 20 h of recovery. (C) Hydrogen peroxide reduces viability in a concentration and time-dependent manner, up to 2 h of exposure. (D) Replication of model assay with positive and negative controls present before, during and after MNNG treatment (viability was quantified 15–20 h post recovery). (E) Replication of model assay with positive and negative controls present during and after MNNG treatment. (F) Replication of model assay with positive and negative controls present only after MNNG treatment. Values shown inside columns (D–F) are normalized, with control viability taken as 100%. Optimization was conducted in HeLa cells and viability was quantified by AB. $^{**}P < 0.01$, $^{***}P < 0.001$ compared with the control; $^{###}P < 0.001$; ns, not significant compared with the effect of MNNG alone. Data shown represent the average of at least four separate experiments or replicates.

the control), consistent with our model. Day-to-day and other variations were minimal and the Z' factor was between 0.5 and 1 (data not shown).

The assay was used to screen the customized library at 1, 10 and 20 µM. At 1 µM, no library compound protected against MNNG (data not shown). At 10 and 20 µM, 4MF and another compound elicited significant concentration-dependent protection against MNNG (Figure 6B, for 10 µM). The second compound was 3',4'-dimethoxyflavone (DMF), which, structurally, is 4MF with an extra methoxy group at

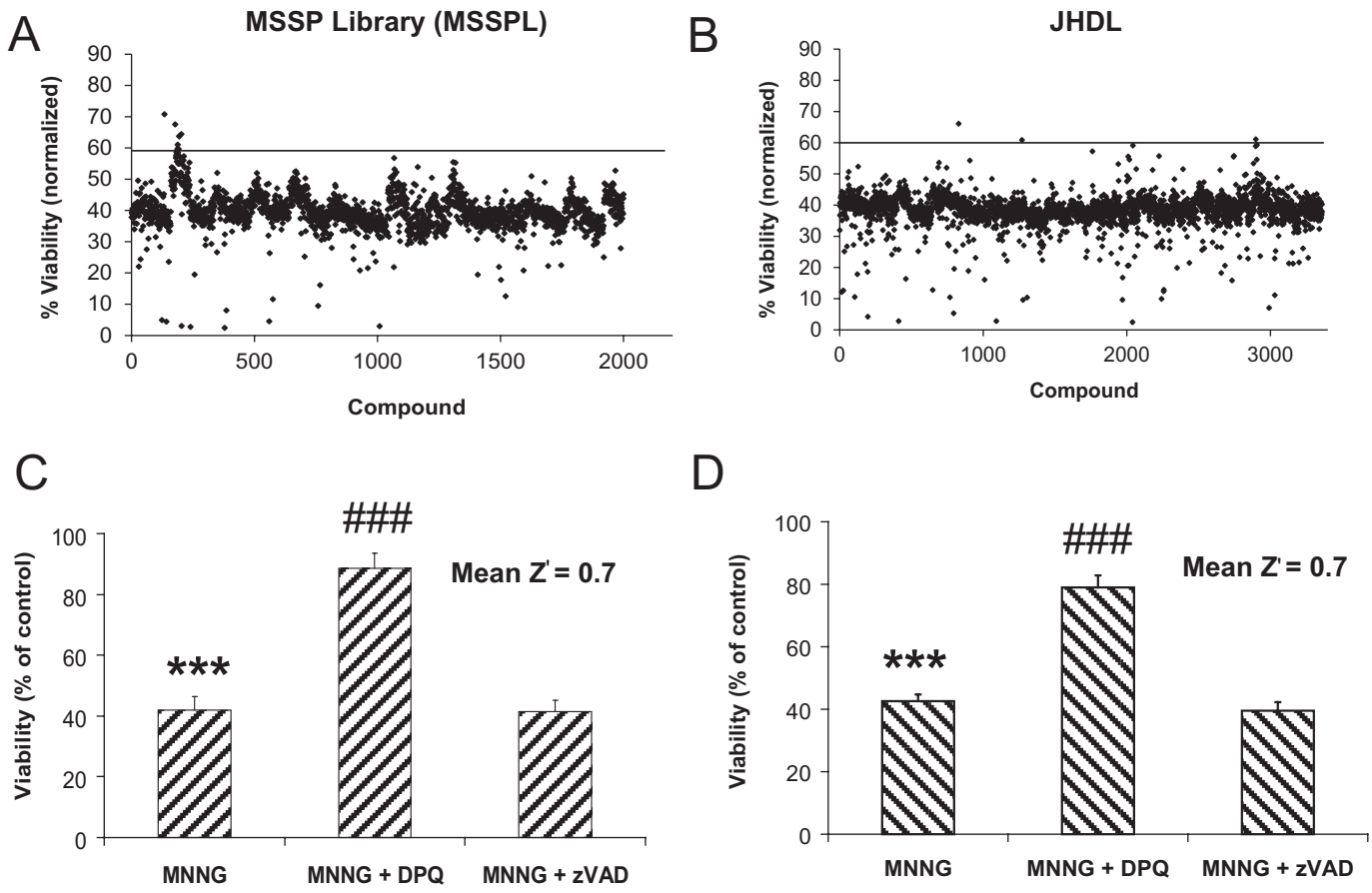

Figure 3

High-throughput screen of chemical libraries. Screening data for (A) MSSPL and (B) JHDL. MSSPL contains 2000 compounds in 25 plates while JHDL has 3120 compounds in 42 plates, making a total of 5120 compounds that were screened. MSSPL was screened robotically while JHDL was screened manually. Values shown represent normalized values after the effect of the toxic stimulus MNNG was set to 40% of the normal control for each plate. A hit was taken as a compound giving a normalized value of at least 60% (indicated by the solid horizontal line in Figure A or Figure B). (C) Pooled data for plates in the MSSPL confirming overall screening replication of the model assay for 22 plates (three plates, numbers 19, 21 and 25, that required rescreening, were excluded). (D) Pooled data for all 42 plates in the JHDL confirming overall screening replication of the model assay. The average Z′ factor for each library was 0.7. ***$P < 0.001$ compared with control; $^{###}P < 0.001$ compared with MNNG alone.

position 3′ of the flavone structure (Figure 4F). Both 4MF and DMF only mildly protected against the reduction in cell viability induced by another toxin, hydrogen peroxide (2 mM, 2 h) (Figure 6C), with the degrees of protection significantly lower than obtained against MNNG, consistent with the fact that they blocked the PARP-1 activation component of the multiple pathways activated by peroxide. To eliminate any cell type-specific artefact, screens against MNNG were run in the dopaminergic SH-SY5Y cells, the data from which were comparable with those obtained in HeLa cells, as both 4MF and DMF at 10 and 20 μM afforded significant protection against the reduction in SH-SY5Y viability induced by MNNG (Figure 6D, for 10 μM).

Concentration–response data for both compounds were then obtained. Again, as observed using the AB assay, the protective effects of both compounds peaked around 25 μM (Figure 7A) and EC_{50} values were determined as 11.41 ± 1.04 μM and 9.94 ± 1.05 μM for 4MF and DMF, respectively (Figure 7B).

4MF and DMF inhibit synthesis and accumulation of PAR polymer

We examined whether 4MF or DMF affects PAR levels. Whereas PAR levels were not detectable in control HeLa cultures treated with DMSO for 5 min, robust PAR levels were found in cultures treated with MNNG, which were not affected by Z-VAD-fmk, but significantly reduced by DPQ. Remarkably, in the presence of 4MF or DMF, levels of PAR induced by MNNG significantly decreased in a concentration-dependent fashion (Figure 7C and D).

4MF and DMF protect against NMDA toxicity in cortical neurones

As our ultimate goal is to find neuroprotective small molecules, we examined the effects of the compounds against neuronal toxicity induced by the overactivation of the NMDA receptor, which is a rallying point for most insults that buffet and eventually kill neurones in the CNS (Fatokun

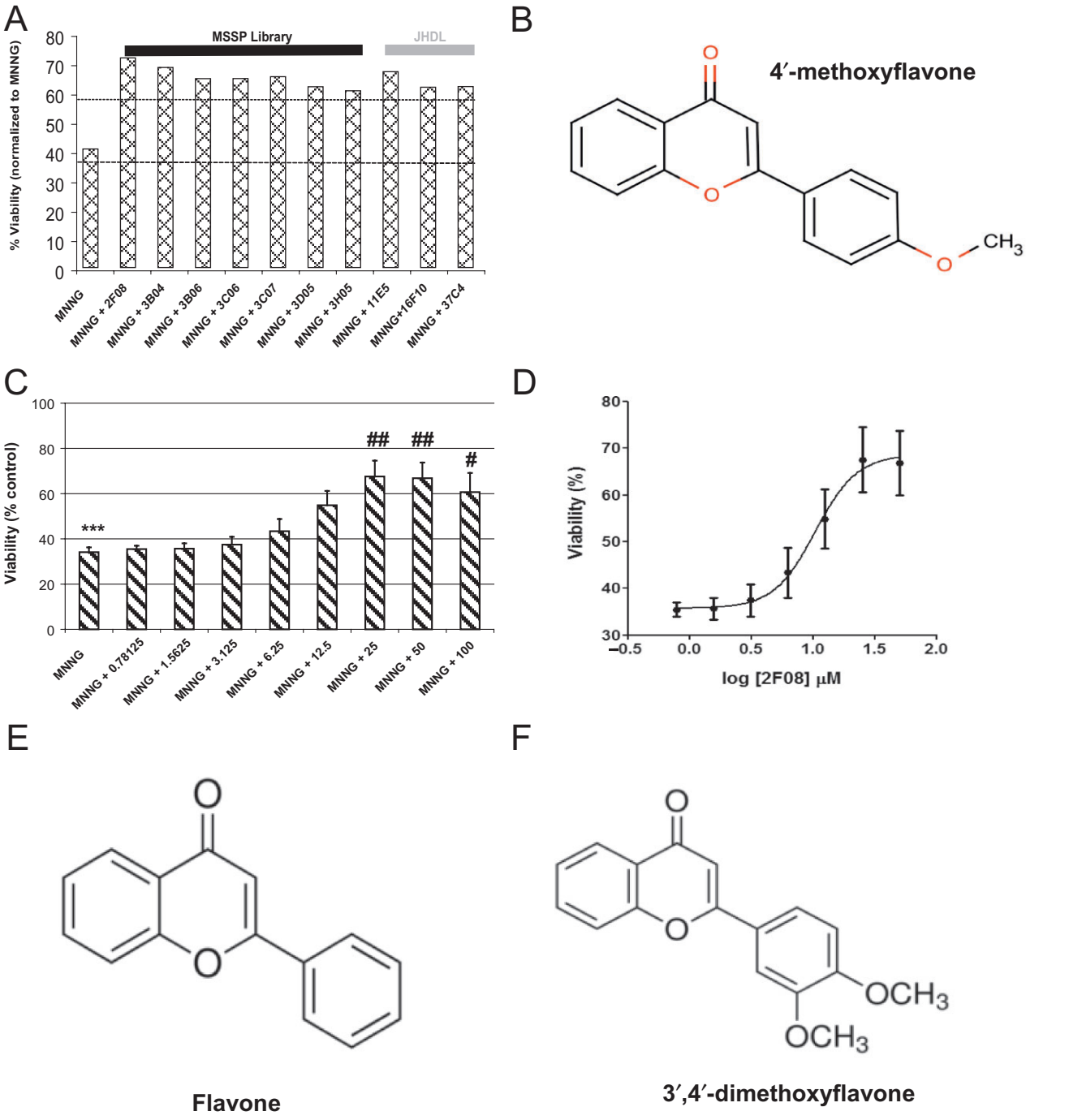

Figure 4

Hit identification and confirmation. (A) Compounds from the two primary screens showing MNNG value-normalized percentage viability of at least 60%. Ten (10) such compounds were identified, seven (7) from the MSSPL (thick, black horizontal line) and three (3) from the JHDL (thick, grey horizontal line). The 40% dotted horizontal line represents normalized MNNG value while the 60% dotted horizontal line represents the minimal level of protection required for a compound to be classified as a hit. Compounds on or above the 60% line were taken as hits. Only one out of the ten compounds, 4MF, was confirmed as a true hit. (B) Chemical structure of 4MF, showing methoxylation (–OCH3) of the parent flavone structure at the 4′ position of the heterocycle. (C) 4MF protects against toxic MNNG effect in a concentration-dependent manner, reaching significance and peaking at 25 μM. Concentrations were chosen in twofold increments up to 100 μM. Numerals on the horizontal axis represent 4MF (2F08) concentrations in μM (100 μM included to demonstrate that effect peaked at 25 μM). (D) Concentration-response data transformed to a sigmoid curve for the determination of EC_{50} value of 4MF (2F08), calculated as 10.41 ± 1.31 μM (GraphPad Prism 5.03; GraphPad Software Inc., San Diego, CA, USA). (E) Chemical structure of the parent compound, flavone. (F) Chemical structure of DMF, showing methoxylation of the parent flavone structure at the 3′ and 4′ positions. Viability was quantified by AB. Values shown in (C) or (D) are for four separate experiments. ***$P < 0.001$ compared with control; $^{\#}P < 0.05$, $^{\#\#}P < 0.01$ compared with MNNG alone.

	Serial number	Flavonoid
Non-flavones	1	Epigallocatechin gallate
	2	Resveratrol
Parent	3	Flavone
Hydroxy-flavones	4	Chrysin (5,7-dihydroxyflavone)
	5	Baicalein (5,6,7-trihydroxyflavone)
	6	Apigenin (5,7,4'-trihydroxyflavone)
	7	Fisetin (3,3',4',7 - tetrahydroxyflavone)
	8	Luteolin (3',4',5,7-tetrahydroxyflavone)
	9	Scutellarein (5,6,7,4'-tetrahydroxyflavone or 6-hydroxyapigenin)
	10	Quercetin (3,5,7,3',4'-pentahydroxyflavone)
	11	Myricetin (3,3',4',5',5',7-hexahydroxyflavone)
Hydroxy-methoxy-flavones	12	Tectochrysin (5-hydroxy-7-methoxyflavone)
	13	Wogonin (5,7-dihydroxy-8-methoxyflavone) - hydrate
	14	Kaempferide (3,5,7-trihydroxy-4'-methoxyflavone)
Methoxy-flavones	15	5-methoxyflavone
	16	7-methoxyflavone
	17	3'-methoxyflavone
	18	***4'-methoxyflavone (lead compound from primary screen)***
	19	3',4'-dimethoxyflavone
	20	7,4'-dimethoxyflavone
	21	5,3'-dimethoxyflavone
	22	5,4'-dimethoxyflavone
	23	5,7-dimethoxyflavone
	24	5,7,4'-trimethoxyflavone
	25	Sinensetin (5,6,7,3',4'-pentamethoxyflavone)
	26	Tangeretin (5,6,7,8,4'-pentamethoxyflavone)
	27	Nobiletin (5,6,7,8,3',4'-hexamethoxyflavone)

Figure 5

Customized flavonoid library for structure–activity relationship study. The library contains 27 compounds, consisting of 2 non-flavone polyphenolic compounds, the parent compound (flavone), 8 compounds carrying only hydroxy-substitutions on the parent compound, 3 compounds with both hydroxy- and methoxy-substitutions, and 13 compounds carrying only methoxy-substitutions on the parent flavone. The substitutions are in varied positions on the ring and are to different degrees. The lead compound, 4MF, is included as an internal control (serial number 18, highlighted). These compounds were initially prepared in DMSO as 10 mM stock solutions, from which 2 mM working stock solutions for screening were prepared.

et al., 2008), with NMDA inducing parthanatos in a cascade of events (David *et al.*, 2009).

Exposure of neuronal cultures to NMDA induced significant neuronal death (parthanatos), compared with cells exposed to control CSS. Death was significantly reduced in the presence of 4MF in a concentration-dependent fashion, bringing the cell-death level to that comparable with the control at the highest concentration tested (100 μM; Figure 8A). Photomicrographs confirmed that cell death in NMDA-treated neuronal cultures was significantly more than in CSS-treated controls and 4MF decreased the cell death, abolishing it at 100 μM (Figure 8B). Similarly, DMF elicited concentration-dependent neuroprotection, although it was less potent than 4MF, with the cell-death level at the three highest concentrations tested significantly lower than that in NMDA-treated cultures, but still significantly higher than in the CSS-treated control cultures (Figure 8C). This was further confirmed by photomicrographs revealing the death-inducing effect of NMDA and the protection afforded by DMF (Figure 8D).

Discussion

This work reports HTS-enabled identification of two novel inhibitors of parthanatos (PARP–1-mediated cell death). Our assay development exploited caspase independency as one of the distinguishing features of our target pathway; and the experimental conditions used in both cell lines and neurones were optimized to specifically induce parthanatos, as earlier reported (Yu *et al.*, 2002). Success in finding these inhibitors demonstrates the capability of the assay to reveal compounds that target parthanatos, even if applied to bigger libraries. The two flavone compounds, 4MF and DMF, belong to the class of plant-derived polyphenolic flavonoids, which have been shown in several studies to possess a broad spectrum of biological activities, including antioxidant, anti-cancer, anti-inflammatory, anti-atherogenic, hypolipidaemic, and neuroprotective or neurotrophic effects (Middleton *et al.*, 2000; Datla *et al.*, 2001; Pan *et al.*, 2002; Kurowska and Manthey, 2004; Nagase *et al.*, 2005a,b).

Earlier reports found methoxyflavones (not 4MF) to have less antioxidant activity than hydroxyflavones or other flavonoids (Arora *et al.*, 1998; Dugas *et al.*, 2000; Takano *et al.*, 2007), although methoxyflavones protected cells against cell death induced by endoplasmic reticulum stress *in vitro* and 1-methyl-4-phenyl-1,2,3,6-tetrahydropyridine injection *in vivo* (a model of Parkinson's disease), whereas hydroxyflavones lacked any protective effect in these conditions (Takano *et al.*, 2007). Methoxyflavones have also been shown to have higher metabolic stability than hydroxyflavones (Walle and Walle, 2007). Our customized library, therefore, afforded the assessment of the potential differential effects of hydroxy- and methoxy-substitutions on the potential ability of the molecules to inhibit parthanatos. Because substitution at the 3′ position alone (3′-methoxyflavone, 3MF) did not produce any protection in our screen, our findings reveal that methoxylation at the 4′ position of the flavone structure may be required for a flavone to inhibit PARP–1-mediated cell death, at least within the range of the low micromolar concentrations tested. We reckon that the protection afforded by 4MF and DMF in our experimental paradigm was not due to their exhibition of any significant antioxidant or free radical-scavenging ability, as there were many compounds in the customized library known to have such properties that did not show any appreciable protection, including epigallocatechin gallate, quercetin and wogonin. Besides, the effects of 4MF and DMF are not thought to have been simply mediated by their better penetration of the cell membranes, as activity by the two compounds was retained across two different cell lines (and in neurones) in which the other flavones in the library with reasonably similar cell membrane penetration profiles showed no activity whatsoever. Most flavonoids and other polyphenols are known to easily penetrate cultured cells; and for most cell culture studies using polyphenolic aglycones (non-glycosides), cellular uptake is not hindered by

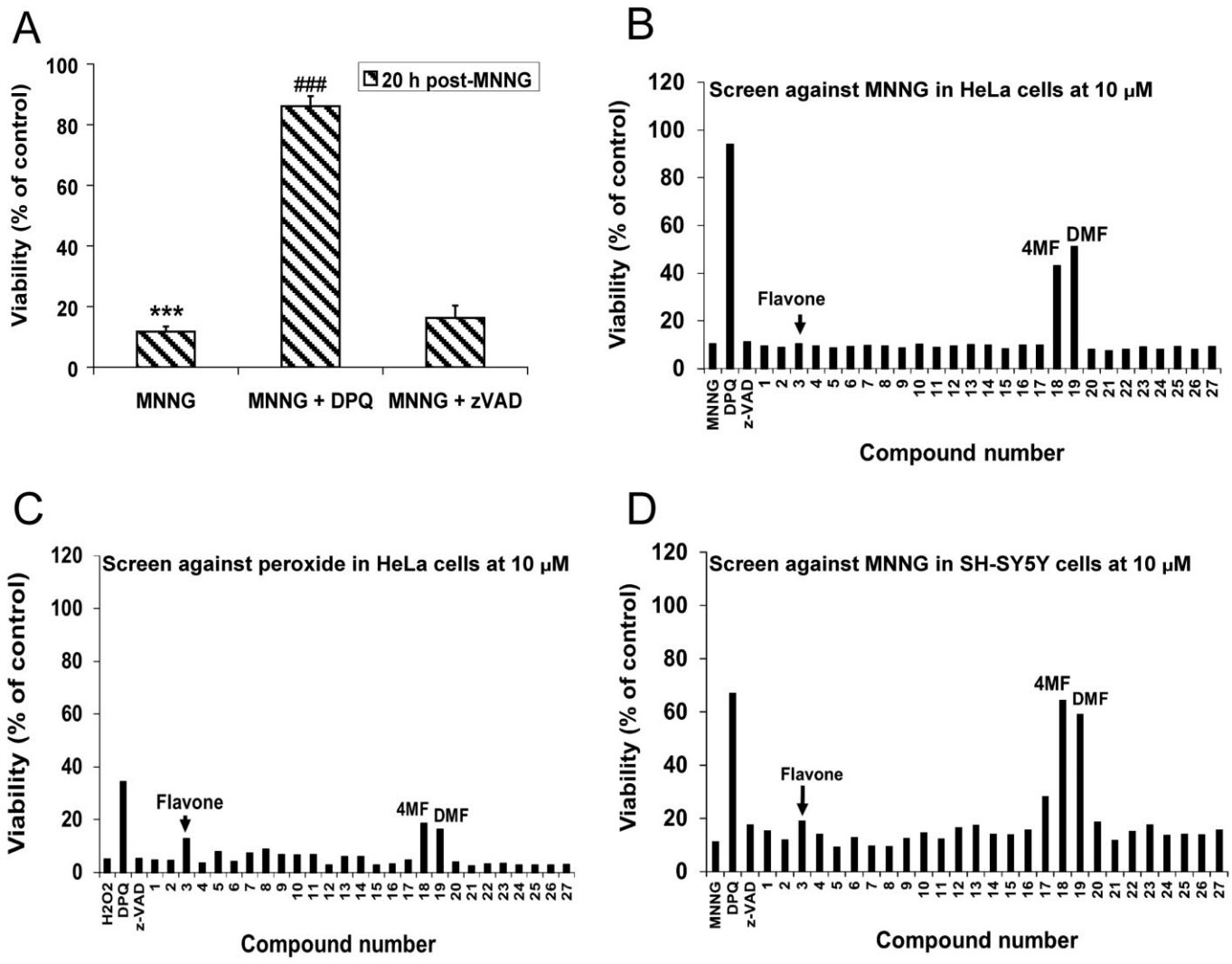

Figure 6

Customized library screen. (A) Model screening assay using luminescence-based CTG for the quantification of cell viability. MNNG reduced cell viability significantly. DPQ protected against the toxic MNNG effect, but z-VAD did not. Quantification was done 15–20 h after 25 min exposure to MNNG followed by restoration to growth medium. (B) Customized library compounds screened at 10 μM against MNNG in HeLa cells. (C) Customized library compounds screened at 10 μM against hydrogen peroxide (H_2O_2) in HeLa cells. (D) Customized library compounds screened at 10 μM against MNNG in dopaminergic SH-SY5Y cells. Arrows, arrowheads or inscriptions show, as indicated, the lack of effect of the parent compound, flavone, the effect of 4MF, or the effect of a second protective compound, DMF. ***$P < 0.001$ compared with control; $^{###}P < 0.001$ compared with MNNG alone. Data in A represent an average of four independent experiments, while B–D show representative data for experiments conducted twice, with similar results obtained in both cases.

poor membrane penetration or efflux transporters and/or metabolic instability (Walle, 2007).

In terms of neuroprotection, 4MF was found to be more potent against NMDA-induced neuronal death than DMF, whereas both compounds were nearly equipotent against MNNG in HeLa and SH-SY5Y neuroblastoma cells, while DMF was more efficacious in HeLa cells, observations that may suggest some subtle differences in the response machinery within neuronal and non-neuronal cells (MNNG induces DNA damage directly while NMDA acts through its receptor, found on neuronal cells). A previous study of the pharmacokinetic disposition of a number of methoxyflavones and hydroxyflavones found that DMF was significantly more stable than 4MF, with its elimination half-life fourfold more than that of 4MF (intrinsic clearance fourfold less), thus placing DMF among the most stable of the methoxyflavones tested, whereas 4MF and 3MF both had comparably poor stability (Walle and Walle, 2007). Therefore, in an *in vivo* setting, the additional methoxylation of 4MF at the 3′ position to produce DMF, while retaining significant ability to inhibit PARP–1-mediated cell death, may significantly enhance metabolic stability, a property that is desirable in drug development.

In this study, the effective concentrations of 4MF and DMF were found to be within the micromolar range. While it remains to be fully clarified why a number of reports have

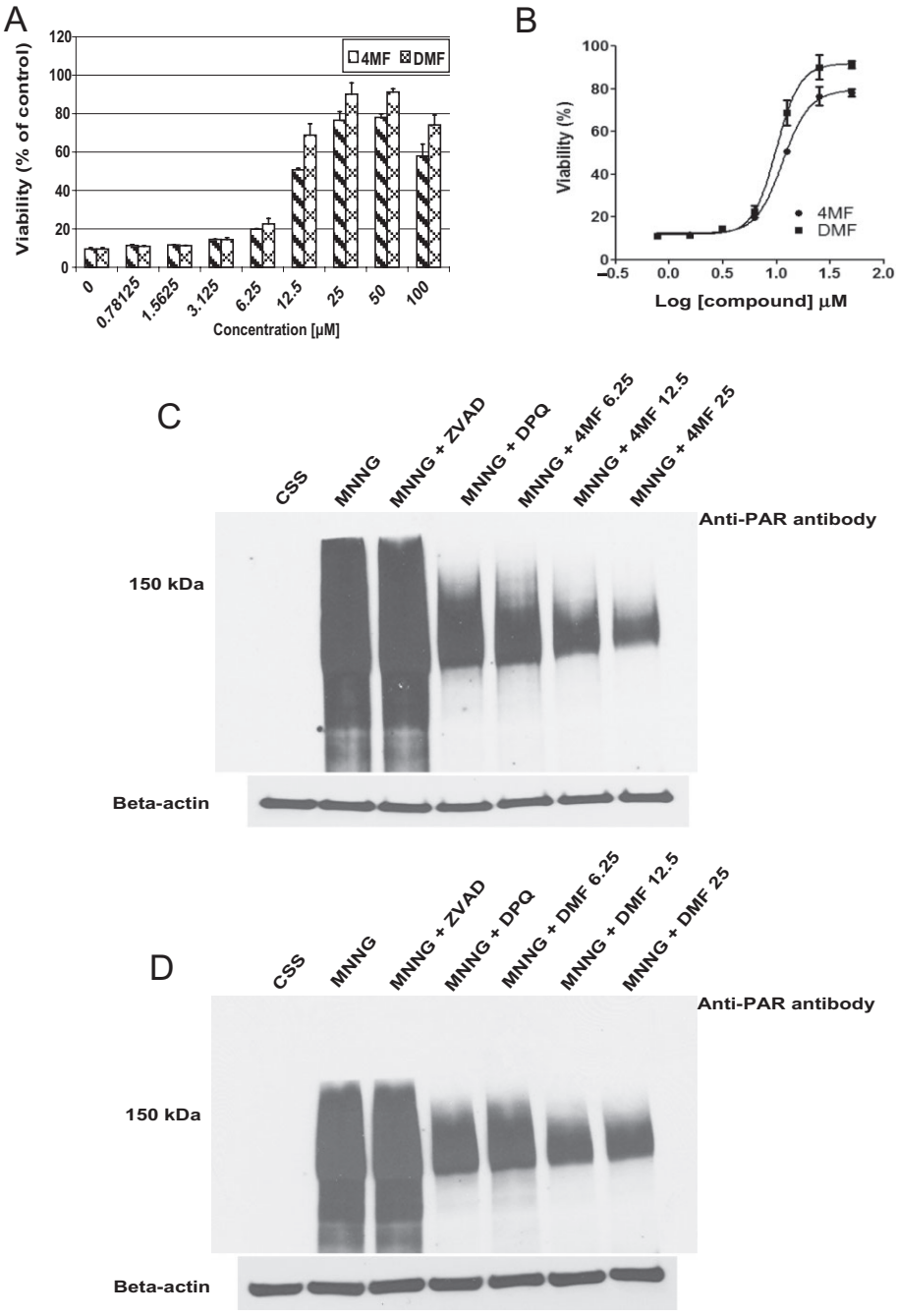

Figure 7

Comparative concentration–response data and inhibition of PAR synthesis and accumulation by 4MF and DMF. (A) Graph showing the concentration-dependent protective effects of 4MF and DMF against MNNG in HeLa cells, with viability quantified by CTG. Values shown are averages of two separate experiments (100 μM shown to demonstrate that effects of the compounds peaked at 25 μM). (B) Concentration–response data in (A) transformed into a sigmoid curve for the determination of EC_{50}. The EC_{50} values are 11.41 ± 1.04 μM and 9.94 ± 1.05 μM, for 4MF and DMF respectively (GraphPad Prism 5.03). (C, D) Assessment of the effects of 4MF and DMF on the levels of PAR polymer induced by MNNG in HeLa cells. Cultures were treated with MNNG (controls treated with DMSO) for 5 min in the presence or absence of increasing concentrations of 4MF or DMF. They were then probed with anti-PAR rabbit polyclonal primary antibody (1:10 000; Trevigen) and, after washing, incubated with anti-rabbit IgG (whole molecule) – peroxidase secondary antibody (1:5000; Sigma). Detection was by chemiluminescence with SuperSignal West Pico Chemiluminescent Substrate (Pierce) and immunoblots were visualized on X-ray films. β-Actin was used as a loading control. Data shown are representative of experiments that were repeated at least three times with similar results.

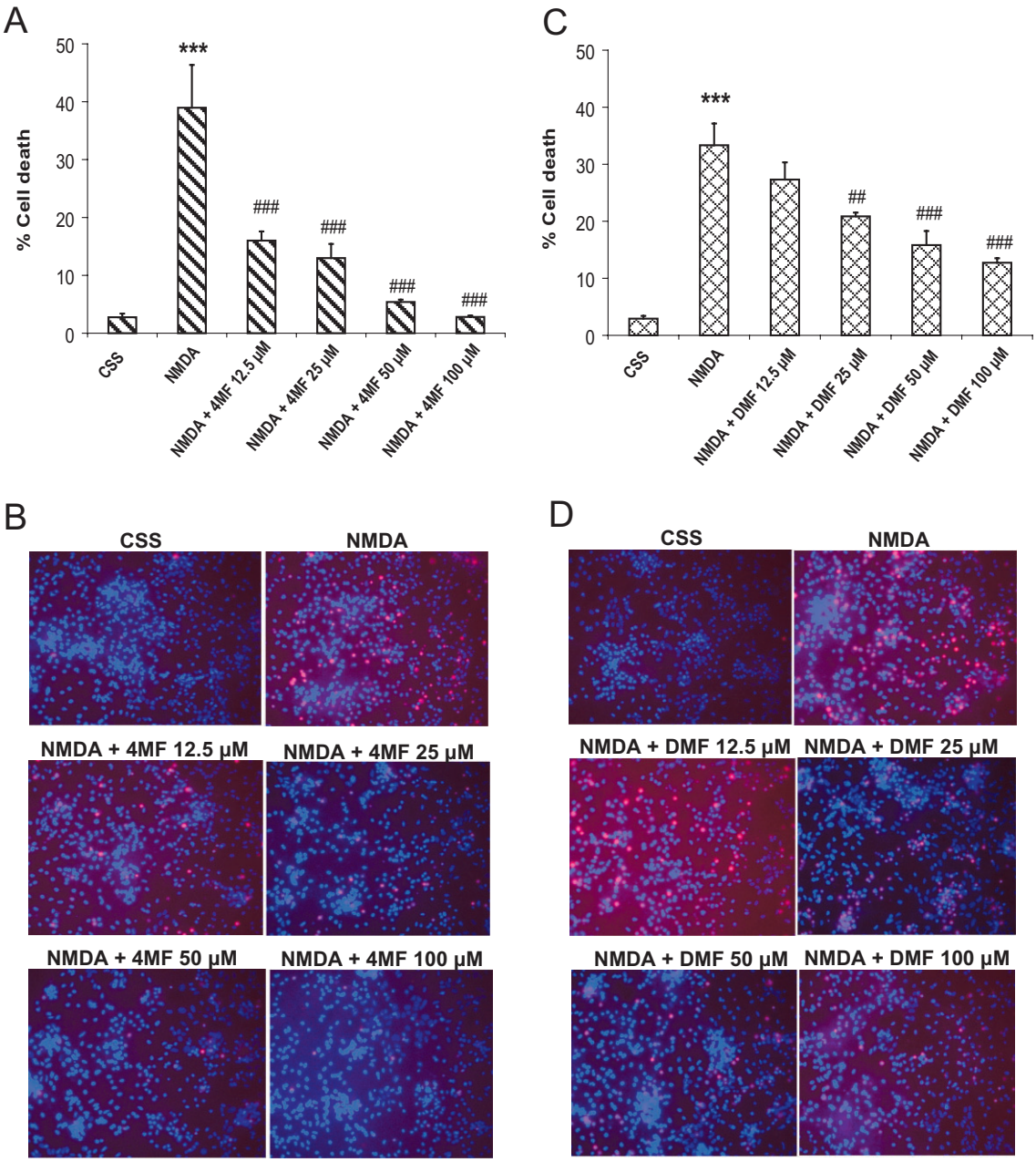

Figure 8

4MF and DMF protect against neuronal death induced by NMDA. Primary neuronal cultures were prepared from gestational day 15–16 fetal CD1 mice. Inhibition of glial proliferation was achieved by addition to the growth medium of 5-fluoro-2′-deoxyuridine (5F2DU, Sigma, 30 µM) at 3–4 days *in vitro*. Cultures so treated represent at least 80% neurones. Cultures were used for experiments at 12–14 days *in vitro*. Control cultures were treated with CSS. NMDA was always freshly prepared in CSS, with 10 µM glycine added to act as a co-agonist at the NMDA receptor. Each treatment was for 5 min. Cultures were then restored to their conditioned growth medium for the next 15–20 h. To assess cell death, cultures were stained with Hoechst 33342 (5 mg·mL^{-1}, labels all cells blue) for 5 min and propidium iodide (1 mg·mL^{-1}, labels dead cells red) for a further 5 min. Medium was then aspirated and cultures washed with CSS before image acquisition after placing the plates on a motorized stage of a Zeiss microscope. Computer-assisted cell counting was then performed with the aid of specialized software (Axiovision 4.6, Zeiss, Germany). At least three separate fields were counted for each treatment. Cell death was calculated as the ratio of PI-stained (red) cells to Hoechst 33342-stained (blue) cells, expressed as a percentage. (A) 4MF concentration-dependently reduced neuronal death induced by exposure to NMDA. (B) Photomicrographs showing dead- and live-cell staining to indicate the death-inducing effect of NMDA on neurones and the concentration-dependent neuroprotective effect of 4MF. Neuroprotection is clearly evident even from the lowest 4MF concentration tested. (C) DMF concentration-dependently reduced neuronal death induced by exposure to NMDA but was less potent than 4MF. (D) Photomicrographs showing dead- and live-cell staining to indicate the death-inducing effect of NMDA on neurones and the concentration-dependent neuroprotective effect of DMF. Neuroprotection is evident with DMF concentration of 25 µM or higher. Data shown are an average of three different fields and are representative of at least three separate experiments with similar results. ***$P < 0.001$ compared with CSS control; $^{\#\#}P < 0.01$, $^{\#\#\#}P < 0.001$ compared with NMDA alone.

described activity for flavonoids at nanomolar range of concentrations against some targets (e.g. see Nilsson *et al.*, 2008; Feng *et al.*, 2010; Cuccioloni *et al.*, 2011), whereas several other reports have only found activity at micromolar range of concentrations, it is possible that the cell type used and the nature of the molecular target(s) in question may explain the differences, at least in part (Fraga and Oteiza, 2011). With regard to what is reported as an attainable physiological concentration for a flavonoid, it should be noted that the plasma concentrations of flavonoids are usually in the nanomolar range, whereas serum concentrations can reach the high micromolar range (Lin *et al.*, 1999; Silberberg *et al.*, 2005; Braidy *et al.*, 2010; Fraga and Oteiza, 2011). The behaviour of a flavonoid in an intact animal depends on its nature (e.g. susceptibility to metabolism) and the target tissue (Walle, 2007). Because methoxyflavones are fairly metabolically stable (especially DMF in this case; Walle and Walle, 2007), their effects *in vivo* may not be mediated by their metabolites to any appreciable extent, if any at all. We reckon that the evidence of activity for 4MF and DMF at the micromolar concentrations examined in this study is consistent with reports of several previous elegant studies conducted in neuronal and non-neuronal cells or tissues, for example (Schroeter *et al.*, 2001; Hanneken *et al.*, 2006; Fernandez *et al.*, 2012), with flavonoid activity against PARP in cell culture models having been almost always reported at micromolar concentrations (Geraets *et al.*, 2007a,b; Braidy *et al.*, 2010; Yashiroda *et al.*, 2010). However, it is possible to obtain, through synthetic chemistry, more potent structural derivatives of the compounds identified in this work that will retain their parthanatos-blocking activity, but regardless of the potency they exhibited, the observation that they both blocked parthanatos at the concentrations used, while other flavonoids in the customized library showed no such activity, makes them attractive as promising pharmacological probes for the study of parthanatos. Of course, a number of PARP-1 inhibitors are commonly used experimentally at micromolar (Garcia *et al.*, 2008; Radnai *et al.*, 2012) or even millimolar (Kuo *et al.*, 1998) concentrations.

Overall, although a series of studies reported a number of flavones to have ability to inhibit PARP-1 in human pulmonary epithelial and vascular endothelial cells (Geraets *et al.*, 2007a,b), our study, as far as we know, is the first to report 4MF and DMF as neuroprotective inhibitors of parthanatos. Although not as potent as most existing PARP-1 inhibitors, they are potentially useful in the pharmacological elucidation of parthanatos. These compounds are to be examined in the near future for their neuroprotective activity in animal models of stroke and neurodegeneration. Our work lends credence to the fact that flavonoids may target specific signalling pathways to elicit their pharmacological actions.

Acknowledgements

The robotic screening component of this work and some aspects of assay optimization were carried out at the ChemCORE Facility of the Johns Hopkins University School of Medicine. We are therefore most grateful to its Director, Prof. Min Li, and the members of staff, especially Dr. Meng Wu and Mr. Alan Long, for their invaluable and generous advice and technical assistance in the execution of the project and for permission to use the Tecan plate reader for the follow-up studies. We also thank Dr. Joong Sup Shim in Prof. Jun Liu's laboratory (Department of Pharmacology, Johns Hopkins University) for his assistance in preparing working stock solutions of the Johns Hopkins Drug Library. Members of the Dawsons laboratory are gratefully acknowledged for their various contributions to the success of this project. This work was generously supported by grants from the NIH/NINDS (NS39148 and NS67525) and the American Heart Association Postdoctoral Fellowship Award to Amos Fatokun (mid-Atlantic affiliate, grant number 0825458E). TMD is the Leonard and Madlyn Abramson Professor of Neurodegenerative Diseases at Johns Hopkins University.

Conflicts of interest

None.

References

Andrabi SA, Kim NS, Yu SW, Wang H, Koh DW, Sasaki M *et al.* (2006). Poly(ADP-ribose) (PAR) polymer is a death signal. Proc Natl Acad Sci U S A 103: 18308–18313.

Andrabi SA, Dawson TM, Dawson VL (2008). Mitochondrial and nuclear cross talk in cell death: parthanatos. Ann N Y Acad Sci 1147: 233–241.

Arora A, Nair MG, Strasburg GM (1998). Structure-activity relationships for antioxidant activities of a series of flavonoids in a liposomal system. Free Radic Biol Med 24: 1355–1363.

Braidy N, Grant R, Adams S, Guillemin GJ (2010). Neuroprotective effects of naturally occurring polyphenols on quinolinic acid-induced excitotoxicity in human neurons. FEBS J 277: 368–382.

Chong CR, Xu J, Lu J, Bhat S, Sullivan DJ, Jr, Liu JO (2007). Inhibition of angiogenesis by the antifungal drug itraconazole. ACS Chem Biol 2: 263–270.

Cuccioloni M, Mozzicafreddo M, Spina M, Tran CN, Falconi M, Eleuteri AM *et al.* (2011). Epigallocatechin-3-gallate potently inhibits the in vitro activity of hydroxy-3-methyl-glutaryl-CoA reductase. J Lipid Res 52: 897–907.

Datla KP, Christidou M, Widmer WW, Rooprai HK, Dexter DT (2001). Tissue distribution and neuroprotective effects of citrus flavonoid tangeretin in a rat model of Parkinson's disease. Neuroreport 12: 3871–3875.

David KK, Andrabi SA, Dawson TM, Dawson VL (2009). Parthanatos, a messenger of death. Front Biosci 14: 1116–1128.

Dawson VL, Dawson TM (2004). Deadly conversations: nuclear-mitochondrial cross-talk. J Bioenerg Biomembr 36: 287–294.

Dawson VL, Dawson TM, Bartley DA, Uhl GR, Snyder SH (1993). Mechanisms of nitric oxide-mediated neurotoxicity in primary brain cultures. J Neurosci 13: 2651–2661.

Dugas AJ, Jr, Castaneda-Acosta J, Bonin GC, Price KL, Fischer NH, Winston GW (2000). Evaluation of the total peroxyl

radical-scavenging capacity of flavonoids: structure-activity relationships. J Nat Prod 63: 327–331.

Fatokun AA, Stone TW, Smith RA (2008). Oxidative stress in neurodegeneration and available means of protection. Front Biosci 13: 3288–3311.

Feng W, Cherednichenko G, Ward CW, Padilla IT, Cabrales E, Lopez JR *et al.* (2010). Green tea catechins are potent sensitizers of ryanodine receptor type 1 (RyR1). Biochem Pharmacol 80: 512–521.

Fernandez SP, Karim N, Mewett KN, Chebib M, Johnston GA, Hanrahan JR (2012). Flavan-3-ol esters: new agents for exploring modulatory sites on GABA(A) receptors. Br J Pharmacol 165: 965–977.

Fraga CG, Oteiza PI (2011). Dietary flavonoids: role of (-)-epicatechin and related procyanidins in cell signaling. Free Radic Biol Med 51: 813–823.

Garcia S, Bodano A, Pablos JL, Gomez-Reino JJ, Conde C (2008). Poly(ADP-ribose) polymerase inhibition reduces tumor necrosis factor-induced inflammatory response in rheumatoid synovial fibroblasts. Ann Rheum Dis 67: 631–637.

Geraets L, Moonen HJ, Brauers K, Gottschalk RW, Wouters EF, Bast A *et al.* (2007a). Flavone as PARP-1 inhibitor: its effect on lipopolysaccharide induced gene-expression. Eur J Pharmacol 573: 241–248.

Geraets L, Moonen HJ, Brauers K, Wouters EF, Bast A, Hageman GJ (2007b). Dietary flavones and flavonoles are inhibitors of poly(ADP-ribose)polymerase-1 in pulmonary epithelial cells. J Nutr 137: 2190–2195.

Hanneken A, Lin FF, Johnson J, Maher P (2006). Flavonoids protect human retinal pigment epithelial cells from oxidative-stress-induced death. Invest Ophthalmol Vis Sci 47: 3164–3177.

Kuo ML, Shen SC, Yang CH, Chuang SE, Cheng AL, Huang TS (1998). Bcl-2 prevents topoisomerase II inhibitor GL331-induced apoptosis is mediated by down-regulation of poly(ADP-ribose)polymerase activity. Oncogene 17: 2225–2234.

Kurowska EM, Manthey JA (2004). Hypolipidemic effects and absorption of citrus polymethoxylated flavones in hamsters with diet-induced hypercholesterolemia. J Agric Food Chem 52: 2879–2886.

Li X, Nemoto M, Xu Z, Yu SW, Shimoji M, Andrabi SA *et al.* (2007). Influence of duration of focal cerebral ischemia and neuronal nitric oxide synthase on translocation of apoptosis-inducing factor to the nucleus. Neuroscience 144: 56–65.

Liang D, Dawson TM, Dawson VL (2004). What have genetically engineered mice taught us about ischemic injury? Curr Mol Med 4: 207–225.

Lin JK, Liang YC, Lin-Shiau SY (1999). Cancer chemoprevention by tea polyphenols through mitotic signal transduction blockade. Biochem Pharmacol 58: 911–915.

Lovborg H, Wojciechowski J, Larsson R, Wesierska-Gadek J (2002). Action of a novel anticancer agent, CHS 828, on mouse fibroblasts: increased sensitivity of cells lacking poly (ADP-Ribose) polymerase-1. Cancer Res 62: 4206–4211.

Middleton E, Jr, Kandaswami C, Theoharides TC (2000). The effects of plant flavonoids on mammalian cells: implications for inflammation, heart disease, and cancer. Pharmacol Rev 52: 673–751.

Nagase H, Omae N, Omori A, Nakagawasai O, Tadano T, Yokosuka A *et al.* (2005a). Nobiletin and its related flavonoids with CRE-dependent transcription-stimulating and neuritegenic activities. Biochem Biophys Res Commun 337: 1330–1336.

Nagase H, Yamakuni T, Matsuzaki K, Maruyama Y, Kasahara J, Hinohara Y *et al.* (2005b). Mechanism of neurotrophic action of nobiletin in PC12D cells. Biochemistry 44: 13683–13691.

Nilsson J, Nielsen EO, Liljefors T, Nielsen M, Sterner O (2008). Azaflavones compared to flavones as ligands to the benzodiazepine binding site of brain GABA(A) receptors. Bioorg Med Chem Lett 18: 5713–5716.

Pan MH, Chen WJ, Lin-Shiau SY, Ho CT, Lin JK (2002). Tangeretin induces cell-cycle G1 arrest through inhibiting cyclin-dependent kinases 2 and 4 activities as well as elevating Cdk inhibitors p21 and p27 in human colorectal carcinoma cells. Carcinogenesis 23: 1677–1684.

Radnai B, Antus C, Racz B, Engelmann P, Priber JK, Tucsek Z *et al.* (2012). Protective effect of the poly(ADP-ribose) polymerase inhibitor PJ34 on mitochondrial depolarization-mediated cell death in hepatocellular carcinoma cells involves attenuation of c-Jun N-terminal kinase-2 and protein kinase B/Akt activation. Mol Cancer 11: 34.

Schroeter H, Spencer JP, Rice-Evans C, Williams RJ (2001). Flavonoids protect neurons from oxidized low-density-lipoprotein-induced apoptosis involving c-Jun N-terminal kinase (JNK), c-Jun and caspase-3. Biochem J 358 (Pt 3): 547–557.

Silberberg M, Morand C, Manach C, Scalbert A, Remesy C (2005). Co-administration of quercetin and catechin in rats alters their absorption but not their metabolism. Life Sci 77: 3156–3167.

Song ZF, Ji XP, Li XX, Wang SJ, Wang SH, Zhang Y (2008). Inhibition of the activity of poly (ADP-ribose) polymerase reduces heart ischaemia/reperfusion injury via suppressing JNK-mediated AIF translocation. J Cell Mol Med 12: 1220–1228.

Sykes ML, Avery VM (2009). Development of an alamar blue viability assay in 384-well format for high throughput whole cell screening of *Trypanosoma brucei* brucei bloodstream form strain 427. Am J Trop Med Hyg 81: 665–674.

Takano K, Tabata Y, Kitao Y, Murakami R, Suzuki H, Yamada M *et al.* (2007). Methoxyflavones protect cells against endoplasmic reticulum stress and neurotoxin. Am J Physiol Cell Physiol 292: C353–C361.

Virag L (2005). Structure and function of poly(ADP-ribose) polymerase-1: role in oxidative stress-related pathologies. Curr Vasc Pharmacol 3: 209–214.

Walle T (2007). Methoxylated flavones, a superior cancer chemopreventive flavonoid subclass? Semin Cancer Biol 17: 354–362.

Walle UK, Walle T (2007). Bioavailable flavonoids: cytochrome P450-mediated metabolism of methoxyflavones. Drug Metab Dispos 35: 1985–1989.

Yashiroda Y, Okamoto R, Hatsugai K, Takemoto Y, Goshima N, Saito T *et al.* (2010). A novel yeast cell-based screen identifies flavone as a tankyrase inhibitor. Biochem Biophys Res Commun 394: 569–573.

Yu SW, Wang H, Poitras MF, Coombs C, Bowers WJ, Federoff HJ *et al.* (2002). Mediation of poly(ADP-ribose) polymerase-1-dependent cell death by apoptosis-inducing factor. Science 297: 259–263.

Yu SW, Wang H, Dawson TM, Dawson VL (2003). Poly(ADP-ribose) polymerase-1 and apoptosis inducing factor in neurotoxicity. Neurobiol Dis 14: 303–317.

Yu SW, Andrabi SA, Wang H, Kim NS, Poirier GG, Dawson TM *et al.* (2006). Apoptosis-inducing factor mediates poly(ADP-ribose) (PAR) polymer-induced cell death. Proc Natl Acad Sci U S A 103: 18314–18319.

Zhang JH, Chung TD, Oldenburg KR (1999). A simple statistical parameter for use in evaluation and validation of high throughput screening assays. J Biomol Screen 4: 67–73.

Zhang X, Chen J, Graham SH, Du L, Kochanek PM, Draviam R *et al.* (2002). Intranuclear localization of apoptosis-inducing factor (AIF) and large scale DNA fragmentation after traumatic brain injury in rats and in neuronal cultures exposed to peroxynitrite. J Neurochem 82: 181–191.

Supporting information

Additional Supporting Information may be found in the online version of this article at the publisher's web-site:

Table S1 Table showing the names, chemical structures and molecular weights of the 27 compounds in the customised secondary screening library. All compounds were purchased from Indofine Chemicals (Hillsborough, NJ, USA), except wogonin, which was purchased from Sigma-Aldrich (St. Louis, MO, USA). The catalogue numbers are as shown underneath the chemical structures.